Diffraction effects in the inelastic scattering of x rays in LiF crystals

V. A. Bushuev, A. V. Laushkin, R. N. Kuz'min, and N. N. Lobanov
M. V. Lomonosov Moscow State University

(Submitted 7 May 1981)

Pis'ma Zh. Eksp. Teor. Fiz. **34**, No. 5, 248–252 (5 September 1981)

A diffractometric study of the interference lines formed as a result of the Bragg diffraction of Compton, Raman, and thermal-diffusion-scattered quanta of MoK_α x radiation in mosaic LiF crystals has been performed. The experimental results are explained within the framework of the theory of secondary extinction.

PACS numbers: 78.70.Ck

The specific characteristics of secondary processes in crystals are attributed to the diffraction of radiation incident on the crystal,[1–3] as well as to the diffraction of secondary radiation; this increases their information content significantly. The secondary processes include, for example, the inelastic scattering (IS) of x rays, electrons, and neutrons, the fluorescent emission by atoms and nuclei, the photoelectric effect, Auger effect and conversion, Cerenkov radiation, etc. The diffraction of x-ray fluorescent radiation and inelastically scattered electrons leads to the formation of Kossel and Kikuchi lines, respectively, in perfect crystals.[4]

Compton scattered (CS) and thermal-diffusion-scattered (TDS) quanta can also experience Bragg diffraction, i.e., elastic coherent scattering. Such a coherent secondary process leads to the appearance of lines with a fine structure in the IS intensity in the directions close to the generatrices of cones with axes along the reciprocal-lattice vectors and half-aperture angles of $90^\circ - \theta_B$, where θ_B is the Bragg angle. The so-called interference Compton lines (ICL) were observed during scattering in diamond mosaic crystals[5] and in compression-deformed and neutron-irradiated LiF crystals.[6] The intensity of the ICL is sensitive to the degree of perfection of the surface layer.[7]

 0021-3640/81/17236-05$00.60

A theory of the Compton effect under the conditions of Bragg diffraction of RS quanta in perfect and mosaic crystals was developed in Refs. 8 and 9.

Photorecording[5-7] does not provide adequate angular resolution for studying the ICL. We have performed the first diffractometric study of the ICL profile for the scattering of MoK_α radiation in LiF crystals, and have also observed the previously unknown lines of the interference Raman effect and interference lines in TDS.

We have studied two LiF samples of different degrees of perfection. The crystals were cut along the (100) planes; the sample thickness was 2 mm and the cross-sectional area was 3×5 mm. The widths of the (200) rocking curves, which were measured on a two-crystal spectrometer in the Laue geometry, were equal to 3.5′ and 11′ for samples 1 and 2, respectively. Sample 2 was pre-irradiated with a thermal-neutron dose of 10^{18} neutrons/cm^2. The MoK_α radiation was monochromatized by reflection from the $(10\bar{1}1)$ planes of bent quartz. The primary beam was incident along the [100] axis; its cross section was 0.13×1.5 mm with a horizontal divergence of 1.2°. The goniometer radius was 143 mm, and the detector slit width was 0.125 mm, consistent with an angular width of 3′. The detector scanned in the equatorial geometry with 3′ intervals.

Figure 1 shows the results of a measurement of the intensity of scattering in the range of angles $\theta \sim 6$–13.5°. The counting rate is ~4 pulses/sec. The ICL corresponding to Bragg reflections of Compton quanta from the (200) planes can be seen near the angle $\theta_B = 10°10'$. The ICL profile is comprised of two adjacent lines with a black and white contrast; the more intense line lies closer to the primary beam.

It can be seen from Fig. 1 that the distance δ between the dark and light lines and the contrast R of the lines increase with increasing disorientation of the mosaic blocks: $\delta = 9'$ and $15'$, $R_{max} = 6\%$, and $R_{max} = 13\%$ for samples 1 and 2, respectively. Such behavior of the ICL can be explained in the following manner. The IS intensity $I(\theta) = I_{RS} + I_{TDS}$ in the observation direction $\theta = \theta_B + \Delta\theta$ decreases by an amount IK because of diffraction, where $K(\Delta\theta)$ is the conversion coefficient in the diffraction direction $\theta_h = -(\theta_B - \Delta\theta)$. The intensity $I(\theta_h)K$ increases in an analogous manner, because of the diffractive transfer of IS quanta from θ_h to the observation direction θ. As a result, the contrast of the interference lines with respect to the incoherent background I is given by

$$R\,(\Delta\theta) = (\tilde{I} - I)/I = -2\,\Delta\theta\,(I'/I)\,K, \tag{1}$$

where $I' = \partial I/\partial\theta$, and I is the IS intensity in which the diffraction is taken into account.

Using the method developed in Ref. 9 within the framework of the theory of secondary extinction, we obtain $K = K_0/\mu l_e$ for mosaic crystals of the first type, where

$$2aK_0 = \frac{y}{a+y}\,e^{-\mu l} - \left[1 - \frac{a}{a+y}\,e^{-y\mu l/\cos\theta_B}\right] e^{-\mu l/\cos\theta_B}. \tag{2}$$

Here $a = 1 - \cos\theta_B$, l is the crystal thickness, μ is the absorption coefficient, $y = 2QW/$

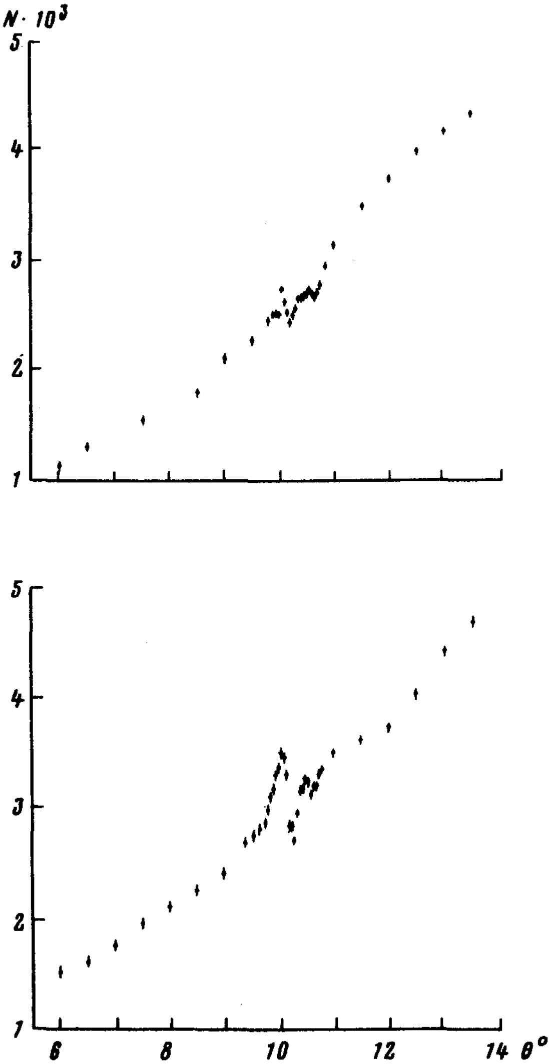

FIG 1. Diffraction patterns obtained for scattering of MoK_α radiation (0.71 Å) in LiF mosaic crystals. Upper spectrum corresponds to sample 1 with a rocking-curve width of 3.5′; the lower spectrum corresponds to sample 2 with a width of 11′.

μ, Q is the total reflection coefficient per unit volume, $W(\Delta\theta)$ is the mosaic distribution function, and l_e is the effective crystal thickness in which the absorption is taken into account.

Calculations using Eqs. (1) and (2) are in good agreement with the observed ICL absorption and the dependence of the contrast and shape of the lines on the mosaic structure. The values $\mu = 3.4\ \text{cm}^{-1}$ and $Q = 1.6 \times 10^{-2}\ \text{cm}^{-1}$ were used, and the width Δ of the mosaic distribution W, which was assumed to be Gaussian, served as the parameter. The RS and TDS cross sections were calculated according to Refs. 10 and 11, from which $I'/I = 6.86$ for $\theta = \theta_B$; this is close to the measured value of 7 ± 0.2. Since $I' > 0$, the contrast is positive for $\Delta\theta < 0$ and negative for $\Delta\theta > 0$. The width of the function K increases with an increase of the block disorientation; therefore, δ and R increase, as was observed in the experiment. After taking into account the corrections for the finite slit and primary beam sizes, we have deduced from the ICL profiles, $\Delta_1 = 4.2'$ and $\Delta_2 = 11.6'$. These values are consistent, within the error limits, with the widths of the mosaic distribution obtained independently from the rocking curves; this indicates that the choice of the model for the formation of the ICL is satisfactory. However, the measured ICL contrasts were more than an order of magnitude greater than the calculated values; this is apparently explained by the finiteness of the primary beam, whereas Eqs. (1) and (2) were obtained in the plane-wave approximation.

The black and white line at $\theta_R = 10°36'$ merits attention. Its location at $\theta_R > \theta_B$ can be explained by the fact that the quanta in the IS spectrum have been displaced downward by an energy $(\theta_R - \theta_B)E \cot\theta_B = 700 \pm 80$ eV. This shift is close to the binding energy of 695 eV for the K electrons of F^-; therefore, we can conclude that the interference Raman effect occurs as a result of IS in which the K electrons of the fluorine ions are excited.

After the passage of the lines near the reflections and spots of TDS $I'_{\mathrm{TDS}} \gg I'_{\mathrm{RS}}$; therefore, their contrast is determined primarily by the TDS contribution. The x-ray patterns indeed revealed black and white interference lines, which clearly "cut through" the TDS holes near the type (113) reflections. After the sample 2 was rotated about the vertical axis by an angle $\theta_B + \phi$, where $\phi = 1.5°$, the diffraction pattern indicated that the (200) TDS spot was intersected by a white line with a contrast $R_{\max} = -32\%$. The negative contrast is explained by the fact that $I(\phi) \ll I_{\mathrm{TDS}}(2\theta_B + \phi)$; therefore, there is almost no influx of quanta from the diffraction direction $\theta_h \approx \phi$. As we move along the interference line, the white contrast in the TDS gradually becomes an ICL with a black and white profile.

Such investigations are important because the location and profile of the interference lines carry information about the crystal structure and its distortions, and also about the spectrum of electron excitations. In the scheme examined by us the crystal scatterer and the crystal analyzer would be combined in one specimen. In this case the energy distribution of the IS quanta is manifested in the angular distribution of the intensity. We also note that Eqs. (1) and (2) are valid for describing the interference lines, which should be observed in the IS of thermal neutrons and mosaic crystals.

1. S. Annaka, J. Phys. Soc. Jpn. 23, 372 (1967); 24, 1332 (1968).
2. V. N. Shchemelev and M. V. Kruglov, Fiz. Tverd. Tela 14, 3556 (1972) [Sov. Phys. Solid State 14, 2988 (1972-73)]; 16, 1472 (1975) [16, 942 (1975)].
3. A. M. Afanas'ev and V. G. Kon, Zh. Eksp. Teor. Fiz. 74, 300 (1978) [Sov. Phys. JETP 47, 154 (1978)].
4. J. Cowley, Fizika difraktsii (Physics of Diffraction), Mir, Moscow, 1979.
5. Y. Yoneda, J. Phys. Soc. Jpn. 16, 1570 (1961).
6. I. V. Telegina and E. V. Kolontsova, Kristallografiya 14, 707 (1969) [Sov. Phys. Crystallogr. 14, 603 (1969-70)].
7. A. V. Laushkin, V. A. Bushuev, R. N. Kuz'min, and N. N. Lobanov, Fiz. Tverd. Tela 23, 278 (1981) [Sov. Phys. Solid State 23, 155 (1981)].
8. V. A. Bushuev and R. N. Kuz'min, Usp. Fiz. Nauk 122, 81 (1977) [Sov. Phys. Usp. 20, 406

(1977)].
9. V. A. Bushuev and R. N. Kuz'min, Kristallografiya **25**, 693 (1980) [Sov. Phys. Crystallogr. **25**, 399 (1980)].
10. G. Palinkas and T. Radnai, Acta Crystallogr. Secr. A **32**, 666 (1976).
11. Y. Kashiwase and Y. Kainuma, J. Phys. Soc. Jpn. **21**, 2663 (1966).

Translated by Eugene R. Heath
Edited by S. J. Amoretty